Physiological variations in CX43 and fibrosis deposition affect human ventricular electrophysiology promoting arrhythmia

Laura García-Mendívil[1], María Pérez-Zabalza[1,2], Ricardo M Rosales[1,3], José M Vallejo-Gil[4], Javier Fañanás-Mastral[4], Manuel Vázquez-Sancho[4], Javier A Bellido-Morales[4], Alexánder S Vaca-Núñez[4], Carlos Ballester-Cuenca[4], Laura Ordovás[1,5], Esther Pueyo[1,3]

[1]Aragón Institute of Engineering Research, University of Zaragoza, IIS Aragón, Zaragoza, Spain
[2]Centro Universitario de la Defensa (CUD), Zaragoza, Spain
[3]CIBER in Bioengineering, Biomaterials and Nanomedicine, Zaragoza, Spain
[4]Department of Cardiovascular Surgery, University Hospital Miguel Servet, Zaragoza, Spain
[5]Fundación Agencia Aragonesa para la Investigación y el Desarrollo (ARAID), Zaragoza, Spain

Abstract

Connexin 43 (Cx43), the major component of gap junctions in the ventricle, is responsible for electrical impulse transmission between ventricular cardiomyocytes. Little is known about the interindividual heterogeneity of CX43 tissue expression in the human left ventricle (LV) and its contribution to arrhythmogenecity either alone or in combination with other proarrhythmic factors like fibrosis. We processed LV fluorescent immunostaining images from living-donors and characterized the population heterogeneity of CX43 expression and fibrosis deposition. The lowest CX43 expression and the highest fibrosis deposition values in the population were implemented in 2D computational models of human LV electrophysiology. We measured conduction velocity (CV) and areas of High Repolarization Gradient (HRG) from the simulated action potentials (APs), and the amplitudes, duration and areas of calculated unipolar electrograms (EGMs). Simulations showed that CV was highly influenced by reduced %CX43, whereas HRG area was more affected by increased fibrosis. The combination of both factors led to the highest decrease in CV, the largest amount of HRG area and the greatest dispersion of repolarization duration (ARI dispersion). In conclusion, decreased %CX43 and increased fibrosis, to extents measured in human LV tissues contribute to a substrate for the generation of reentrant arrhythmias, which can be quantified from ventricular EGMs.

1. Introduction

Cx43 is the major component of ventricular gap junctions, the intercellular communication structures responsible for ion and small molecule exchange and electrical coupling between adjacent cardiomyocytes. Ventricular electrical coupling can be affected by changes in Cx43 expression and/or distribution. These changes can lead to impulse conduction abnormalities and arrhythmias, especially when combined with other structural and functional changes related to pathological remodeling or aging. Altered CX43 patterns have been reported in humans with left ventricular hypertrophy, heart failure, atrial fibrillation and dilated cardiomyopathy [1]. However, little is known about the physiological variability of CX43 expression among individuals in non-diseased human left ventricle (LV) and its associated arrhythmic risk. Cardiomyocytes are embedded in the extracellular matrix, which provides cell support, tissue strength and enables cell-to-cell communication. Increased fibrosis deposition has been reported to alter the electromechanical function of the heart and increase proarrhythmicity [2,3]. In the literature, there is limited research on the impact that the combination of alterations in CX43 and fibrosis has on human ventricular electrophysiology.

Here, we report our experimental characterization of CX43 amount in human LV tissues from a middle-age to elderly population. Next, we evaluate the effects of the different amounts of CX43 on human LV electrophysiology, both individually and combined with increased fibrosis deposition, using 2D computational models. We investigate how those effects can be associated with arrhythmic risk and how they can be detected from ventricular unipolar electrograms (EGM).

2. Methods

2.1. Human LV tissues

Human transmural LV tissue sections (n=44) were collected at Hospital Universitario Miguel Servet (Zaragoza,

Spain) from 50 to 84 year-old patients undergoing cardiac surgery. They all fulfilled clinical criteria, including absence of hypertrophy and prior myocardial infarction and preserved LV ejection fraction, among others. The samples were obtained during cardiac arrest, immediately after the patient was placed on cardiopulmonary bypass, from an area of the anterior wall of the LV, near the base of the heart, without evidence of ischemia or any other macroscopic pathology [4].

2.2. Fluorescent immunohistochemistry

Standard immunohistochemistry protocols were used for tissue staining. Primary antibodies were mouse monoclonal anti-SERCA2 (ab2817, Abcam) and rabbit polyclonal anti-CX43 (ab11370, Abcam). Secondary antibodies were Alexa Fluor 488 goat anti-mouse (A11029, Thermo Fisher) and Alexa Fluor 633 goat anti-rabbit (A21071, Thermo Fisher). The extracellular matrix was stained with wheat germ agglutinin (WGA) conjugated to Alexa Fluor 555 (W32464, Thermo Fisher). Images were acquired with a Zeiss LSM 880 (Carl Zeiss) confocal microscope.

2.3. CX43 and fibrosis characterization

Binary masks for CX43, SERCA2 and WGA were generated by applying a binarization filter to grayscale images. The amount of CX43 (%CX43) was calculated as the percentage of CX43 with respect to the area of the cardiomyocytes measured from the SERCA2 mask. The quantification of fibrosis was performed using WGA staining after substracting the sarcolemma signal labeled by SERCA2 [3].

2.4. Computational simulations

We defined a two-dimensional computational model of human LV electrophysiology consisting of epicardial and midmyocardial regions, as illustrated in Figure 1A. The O'Hara-Rudy model [5] was used to describe the human ventricular action potential (AP) for the epicardial and midmyocardial cells. The control case was defined with a longitudinal diffusion coefficient of 0.0013 cm^2/ms and a transverse-to-longitudinal conductivity ratio of 0.19. Three other cases were simulated to represent the lowest values of %CX43 and the largest amounts of fibrosis measured from the LV tissues. In the fibrosis case (hereafter, FIB), 19% of the tissue elements were uniformly randomly selected to represent fibrotic elements and were represented by the MacCannell AP model [6]. The longitudinal conductivity between fibroblasts and myocytes was reduced by a factor of three. The diffusion case (hereafter, DIF) was implemented by reducing the longitudinal conductivity by 40%. The fibrosis plus diffusion case (hereafter, FIB+DIF) combined the two previous cases. Simulations were run using ELECTRA, an in-house cardiac electrophysiology solver. The finite element method was used to solve the cardiac monodomain model [3].

AP duration (APD) was computed at 90% repolarization. Local repolarization gradients were computed, for each mesh node, as the magnitude of the repolarization gradient vector, estimated using a radius of one pixel [7]. We calculated the percentage of tissue area with repolarization gradients above 9 ms/mm, termed High Repolarization Gradient (HRG) area. For Conduction Velocity (CV) estimation, we fitted a polynomial surface to the activation data and we calculated the local velocity vectors from the gradient of the fitted surface [8].

2.5. Analysis of electrograms

Unipolar EGMs were computed from a 9x9 electrode mesh located in the center of the tissue at a distance of 0.1 cm. The inter-electrode distance was 0.2 cm. For an electrode located at a position **r'**, the EGM ϕ_e (**r'**,t) was computed as:

$$\phi_e(\mathbf{r'}, t) = \int\int \left[-\nabla_r V_m(\mathbf{r}, t) \cdot \nabla_r \left(\frac{1}{d(\mathbf{r}, \mathbf{r'})} \right) \right] dxdy \quad (1)$$

$$\mathrm{d}(\mathbf{r}, \mathbf{r'}) = \|\mathbf{r} - \mathbf{r'}\|_2 \quad (2)$$

where **r** = [*x y z*] and **r'** = [*x' y' z'*] are the Cartesian coordinate vectors for a point in the tissue and the electrode, respectively, and ∇_r denotes the spatial gradient. The integral was calculated over the whole 2D tissue in the x-y plane [9].

For each EGM, the following markers were measured:

Activation Recovery Interval (ARI). ARI was calculated as the interval between activation time (AT) and repolarization time (RT). AT and RT were defined from the minimum and maximum derivatives, respectively, in predefined intervals of the last simulated heartbeat after a train of periodic stimuli at a pacing frequency of 1 Hz. Two measures of repolarization dispersion were evaluated: ARI_d, defined as maximum ARI - minimum ARI from the 81 calculated EGMs; and ARI_{std}, defined as the standard deviation of ARI measures from the 81 EGMs (Figure 1).

T-wave amplitude (R_A): Maximum absolute value of the repolarization wave corresponding to a positive or a negative peak, computed following the method described in [9].

Peak-to-peak voltage (V_{QRS}): Difference between maximum and minimum voltage in the EGM activation wave.

QRS (S_{QRS}) and T-wave (S_T) areas: Integrated areas over the depolarization and repolarization waves of the EGM, respectively. The areas were normalized by the

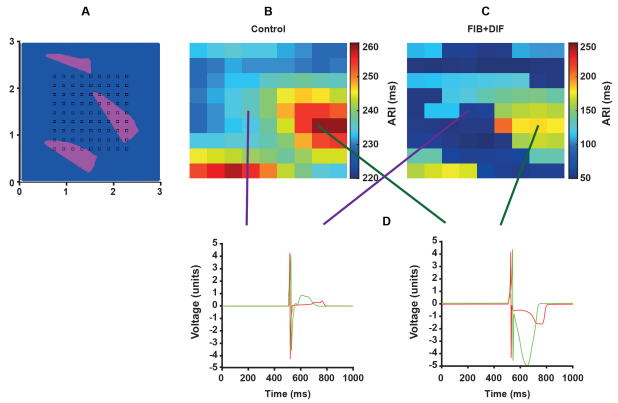

Figure 1: A) 2D tissue model with epicardial cells in blue and midmyocardial cells in pink, and array of electrodes for EGM calculation. ARI map for control (B) and FIB (C) cases. D) EGMs for two electrodes computed for control (red) and FIB (green) cases.

difference between the maximum and minimum EGM amplitudes.

3. Results and Discussion

3.1. CX43 and fibrosis in human LV tissues

The median [interquartile range] of CX43 amount, %CX43, in the population was 2.73% [1.93%-3.52%]. Some individuals had 40% lower %CX43 than the population median, indicating high interindividual variability. For fibrosis deposition, the median [interquartile range] in the population was 10.44% [8.33%-13.65%]. The greatest fibrosis deposition in the population was 19%.

In the computational models, the DIF case represented 40% decrease in %CX43 relative to the population median (implemented by decreased longitudinal conductivity) and the FIB case included 19% fibrosis deposition.

3.2. CX43 and fibrosis effects on tissue APs

We observed a decrease in CV in the FIB case and this was even more accentuated in the DIF case, in association with the reduced conduction between fibroblasts and cardiomyocytes in the FIB case and to the low longitudinal conductivity in the DIF case. The combination of both factors (FIB+DIF) resulted in a higher CV reduction. HRG, considered as a measure of repolarization dispersion and a surrogate for arrhythmic risk [7], was increased in FIB, DIF and FIB+DIF, particularly in FIB+DIF. HRG results suggest that both reduced %CX43 and increased fibrosis, and especially their combination, may contribute to a more proarrhythmic susbtrate (Figure 2). Altogether, the increased heterogeneity in repolarization duration, and thus in the effective refractory period, combined with reduced CV, as observed in some individuals of our population with non-pathological LV remodeling, can promote the generation of reentrant arrhythmias.

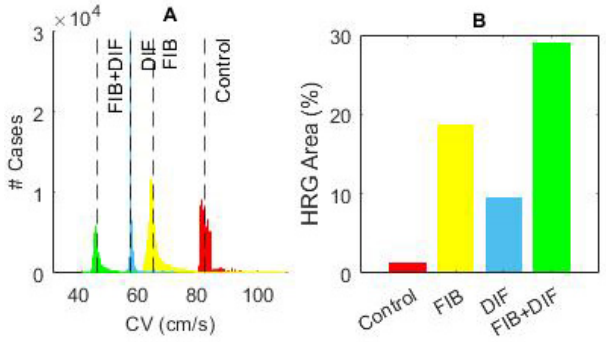

Figure 2: A) CV and B) HRG area for control, FIB, DIF and FIB+DIF simulated cases. Dashed lines represent the median of each case.

3.3. CX43 and fibrosis effects on EGMs

The reduction in CV for FIB, DIF, and FIB+DIF cases could also be quantified from the ATs estimated from the simulated EGMs. We additionally characterized V_{QRS} and S_{QRS} in the four cases. We observed a strong decrease in V_{QRS} for the FIB case and an increase in V_{QRS} for the DIF case. The combined FIB+DIF case resulted in a slight decrease with respect to control (Figure 3A). For the normalized area S_{QRS}, we observed an increase in the three cases, especially in DIF and FIB+DIF cases (Figure 3B). S_{QRS} is dependent on both the amplitude and duration of the EGM activation waveform, and both reduced %CX43 and increased fibrosis led to delayed conduction, which combined with the effects on V_{QRS}, led to an increase in the S_{QRS}.

With respect to EGM repolarization, R_A was increased in all three simulated cases. This effect can be attributed to the heterogeneities already present in the control case, with islands of midmyocardial cells embedded in an epicardial tissue. We observed that the presence of fibrosis in a homogeneous tissue with only epicardial cells decreased R_A, in line with previous studies in the literature. In our heterogeneous tissue, which could more closely resemble the heterogeneity of LV tissues, an increase in the median R_A over all calculated EGMs could be seen, despite a high number of repolarization waves presenting negative amplitudes compared to the control case, especially in FIB and FIB+DIF cases (Figure 3C).

For the normalized area S_T, we observed a noticeable increase in FIB, DIF, and FIB+DIF cases with respect to control (Figure 3D). This could be indicative of higher local

heterogeneity of ventricular repolarization.

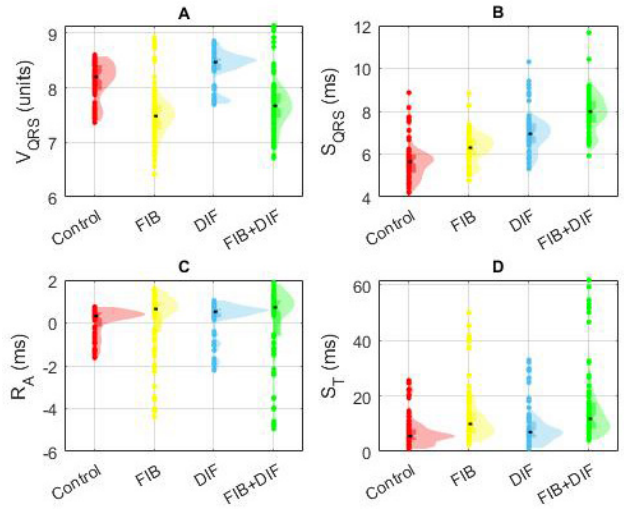

Figure 3: A) V_{QRS}, B) V_{QRS}, C) R_A and D) S_T for control, FIB, DIF and FIB+DIF simulated cases. Black lines represent the median.

Regarding measures of ARI dispersion, we found that DIF and especially FIB and FIB+DIF led to a large increase in both ARI_d and ARI_{std} (Table 1). This increased spatial variability in repolarization duration, combined with the reduction in CV observed in FIB+DIF, could result in increased susceptibility to reentrant arrhythmias.

Table 1: Repolarization dispersion measures, ARI_d and ARI_{std}, evaluated in control, FIB, DIF and FIB+DIF simulated cases.

Scenario	ARI_d (ms)	ARI_{std} (ms)
Control	30	8.59
FIB	116	43.58
DIF	39	10.42
FIB+DIF	155	46.50

The effects of physiological remodeling of %CX43 to the extent observed in our population of donors with non-diseased LV tissues, has profound effects on cardiac electrophysiology, particularly when combined with increased fibrosis deposition. Such effects are manifested in unipolar ventricular EGMs by alterations in features related to both depolarization and repolarization.

4. Conclusions

A low amount of CX43 and high fibrosis deposition to extents observed in non-diseased human LV tissues have remarkable effects in CV and repolarization dispersion, enhancing the vulnerability to arrhythmias. Such effects can be quantified from the analysis of the amplitude, duration and areas of the depolarization and repolarization waves of ventricular EGMs.

Acknowledgments

This work was supported by AEI-Ministerio de Ciencia e Innovación (PID2019-105674RB-I00, TED2021-130459B-I00, PID2022-140556OB-I00 and PID2022-139859OB-I00 funded by MCIN/10.13039//501100011033 and by "ERDF A way of making Europe"), by Gob. Aragón (LMP94_21, LMP128_21 and BSICoS group T39_23R) and by European Research Council (G.A. 638284).

References

[1] Salameh A, et al. The signal transduction cascade regulating the expression of the gap junction protein connexin43 by beta-adrenoceptors. Br J Pharmacol Sept 2009;158(1):198–208.

[2] Ramos-Marques E, et al. Chronological and biological aging of the human left ventricular myocardium: analysis of micrornas contribution. Aging Cell Jul 2021;20(7):e13383.

[3] Garcia-Mendivil L, et al. Analysis of age-related left ventricular collagen remodeling in living donors: Implications in arrhythmogenesis. iScience Jan 2022;25(2):103822.

[4] Oliván-Viguera A, et al. Minimally invasive system to reliably characterize ventricular electrophysiology from living donors. Sci Rep Nov. 2020;10(1):19941.

[5] O'Hara T, et al. Simulation of the undiseased human cardiac ventricular action potential: Model formulation and experimental validation. PLoS Comput Biol 2011;7(5):e1002061.

[6] MacCannell KA, et al. A mathematical model of electrotonic interactions between ventricular myocytes and fibroblasts. Biophys J Jun. 2007;92(11):4121–4132.

[7] Mendonca-Costa C, et al. Pacing in proximity to scar during cardiac resynchronization therapy increases local dispersion of repolarization and susceptibility to ventricular arrhythmogenesis. Heart Rhythm Oct 2019;16(10):1475–1483.

[8] Bayly PV, et al. Estimation of conduction velocity vector fields from epicardial mapping data. IEEE Trans Biomed Eng May. 1998;45(5):563–571.

[9] Celotto C, et al. Location of parasympathetic innervation regions from electrograms to guide atrial fibrillation ablation therapy: An in silico modeling study. Frontiers in Physiology Aug 2021;12:674197.

Address for correspondence:

Laura García-Mendívil
Universidad de Zaragoza, Campus Río Ebro, Edif.I+D, C/ Poeta Mariano Esquillor, s/n, 50018 Zaragoza
lgmendivil@unizar.es